A New Time-Domain Macromodel for Transient Simulation of Uniform/Nonuniform Multiconductor Transmission-Line Interconnections*

Monjurul Haque, Ali El-Zein†, S. Chowdhury‡
University of Iowa, Iowa City, IA 52242

Abstract: A rational-function hybrid-parameter model for general multiconductor transmission lines is derived from a spectral-method solution of the telegrapher equations, using Chebyshev polynomials to represent spatial variation. Time-domain macromodel is then generated by a recursive convolution algorithm which can be simulated efficiently with arbitrary terminations. Results from a transient simulator implementing the approach are presented to demonstrate the accuracy, efficiency and stability of the derived macromodel.

I. INTRODUCTION

Today's high-speed logic families, with subnanosecond switching speeds, demand that the physical interconnections such as in multichip modules and printed circuit boards conform with the results of distributed-element theory. The design of state-of-the-art VLSI circuits, therefore, requires accurate and efficient simulation tools for transmission lines (modeling interconnections) terminated in linear/nonlinear networks.

Among numerous simulation techniques available, one approach [1]-[5] solves the telegrapher equations (associated with general transmission lines) in the frequency domain. Inverse fast Fourier transform or numerical (analytical in some cases [5]) inverse Laplace transform is then used to transform the frequency-domain data into an equivalent time-domain description (known as the impulse-response or Green's function). The dynamic interaction of the transmission line with the terminal networks is evaluated by convolving the impulse-response with the port variables. The long duration of the impulse response often requires computation that increases quadratically with the simulation time. The numerical inverse transform techniques require numerous samples of the frequency-domain function. In addition, some of the frequency-dependent matrix parameters have wide frequency spectrums and often do not become zero as the frequency approaches infinity. The high-frequency limiting values of these parameters cannot, in general, be determined analytically. Consequently, the band-limiting action of the inverse transform techniques will introduce ringing and aliasing error in the impulse response data.

To avoid the time-consuming direct convolution, a recursive convolution technique has been developed [6] that requires the impulse-response to be expressed as sum of exponentials in time domain (i.e. rational-function approximations in s-domain, s being the Laplace transform variable). Pade approximation (and a moment matching technique) used for this purpose [7]-[9] has limited accuracy and often suffers from the instability problem in the form of right-half plane poles. Modifications, such as enhanced moment matching [10] and multi-point moment matching [11], cannot be extended to include nonuniform transmission lines in the absence of a generalized moment computation technique and because of the aforementioned stability problem [12]. An alternative recursive convolution formulation employing exponentially decaying polynomial approximations (for the impulse-response [12]) guarantees stable impulse-response, and is applicable to nonuniform lines and frequency-varying parameters but requires large number of samples of the frequency-domain function to achieve high accuracy.

This paper describes a spectral method with Chebyshev polynomials as the basis functions to solve the s-domain telegrapher equations. Chebyshev expansion, representing the spatial variation [13], provides an accurate time-domain solution for the general transmission line problem but requires the computationally expensive evaluation of a matrix exponentials at each time step. In this work, the accuracy and generality of the spectral technique are fully exploited to derive a frequency-dependent h-parameter description of a transmission line. The formulation also yields a rational function expansion for the h-parameter network function in partial fraction form. In addition, a common set of poles is generated for all the elements of the h-parameter matrix which greatly simplifies the transient simulation scheme. The extracted rational function model and a recursive convolution algorithm are then used to construct a time-domain macromodel that can be easily implemented in a circuit simulator. The macromodel can also be incorporated as a submatrix in the MNA (modified nodal analysis) matrix of the overall circuit. The advantages of the proposed method over the other techniques are in its generality, flexibility, computational stability and its compatibility with conventional circuit simulators such as SPICE. The method permits the construction of a macromodel of arbitrary order without experiencing the instability problem inherent in Pade approximation and is general in that it is applicable to both uniform and nonuniform lines. It can provide SPICE-like accuracy at a speed comparable to the techniques that employ Pade approximation.

Section II describes the spectral method used to obtain an s-domain h-parameter representation of a transmission line system. Section III describes the macromodel and the transient simulation scheme based on recursive convolution of impulse-response with piecewise-linear port voltage and current waveforms. The implementation of the approach in a prototype transient simulator TRAIN is also described. In Section IV, representative examples are presented to illustrate the accuracy and efficiency of the method. Conclusions and suggestions for future work are presented in Section V.

II. TRANSMISSION LINE HYBRID PARAMETER MATRIX

The telegrapher equations in the s-domain for a system of N-conductor transmission lines can be written in matrix form as

$$\frac{d}{dx}\begin{bmatrix}\mathbf{V}(x,s)\\ \mathbf{I}(x,s)\end{bmatrix} = -\begin{bmatrix}\mathbf{0} & \mathbf{R}(x)+s\mathbf{L}(x)\\ \mathbf{G}(x)+s\mathbf{C}(x) & \mathbf{0}\end{bmatrix}\begin{bmatrix}\mathbf{V}(x,s)\\ \mathbf{I}(x,s)\end{bmatrix} \quad (1)$$

* This research was supported by the National Science Foundation under its grant MIP-9003434. † Ali El-Zein is now with IBM, Poughkeepsie, NY. ‡ S. Chowdhury is now with Motorola, Austin, TX.

where $\mathbf{V}(x,s)$ and $\mathbf{I}(x,s)$ are, respectively, the voltage and current vectors of length N; $\mathbf{R}$, $\mathbf{L}$, $\mathbf{C}$, and $\mathbf{G}$ are, respectively, the per-unit-length resistance, inductance, capacitance and conductance matrices. The per-unit-length parameters are functions of the distance coordinate x for nonuniform lines.

In general, (1) can not be solved analytically. The Chebyshev expansions of $\mathbf{V}(x,s)$ and $\mathbf{I}(x,s)$ with respect to the spatial variable x will be used to formulate a numerical solution to (1). The properties of Chebyshev polynomials, such as orthogonality, greatly facilitates the mathematical formulation. Since Chebyshev polynomials are defined on the interval [-1,+1] whereas transmission-line problems are usually formulated in the interval $[0, \ell]$, a change of variable $x' = 2x/\ell - 1$ is necessary. The transformed equation is

$$\frac{d}{dx'}\begin{bmatrix}\mathbf{V}(x',s)\\ \mathbf{I}(x',s)\end{bmatrix} = -\frac{1}{2}\ell\begin{bmatrix}\mathbf{0} & \mathbf{R}(x')+s\mathbf{L}(x')\\ \mathbf{G}(x')+s\mathbf{C}(x') & \mathbf{0}\end{bmatrix}\begin{bmatrix}\mathbf{V}(x',s)\\ \mathbf{I}(x',s)\end{bmatrix} \tag{2}$$

A transmission-line system with N conductors can be considered as a 2N-port linear network. The h-parameter representation of the network can be written as

$$\begin{bmatrix}\mathbf{V}(+1,s)\\ \mathbf{I}(-1,s)\end{bmatrix} = \mathbf{H}(s)\begin{bmatrix}\mathbf{V}(-1,s)\\ \mathbf{I}(+1,s)\end{bmatrix}, \tag{3}$$

where $\mathbf{H}(s)$ is the frequency-dependent hybrid parameter matrix. In order to evaluate $\mathbf{H}(s)$ as a function of s, each per-unit-length parameter is expanded in a Chebyshev series. Truncation of the series gives a finite degree polynomial with minimal maximum error for the chosen number of terms [14]. Substituting these expansions for per-unit-length parameters, voltage and current in (2) and requiring the weighted error to be orthogonal with the approximating Chebyshev polynomials, a set of algebraic equations for the undetermined expansion coefficients are obtained. The solution of the related matrix equation is then used to calculate the frequency-dependent h-parameter matrix. To simplify the description, the case of a single-conductor line will be described. Extension to a multiconductor-line system is straightforward.

2.1. Hybrid parameters of a single transmission line

For a single-conductor line, the vectors in (2) are replaced by the corresponding scalars V, I, R, L, C and G. Here and in what follows, the dependence of the line voltage and current on the Laplace transform variable s will be suppressed for notational convenience. The Chebyshev expansions are as follows:

$$R(x') = \sum_{k=0}^{N_C-1}{}' r_k T_k(x'), \qquad L(x') = \sum_{k=0}^{N_C-1}{}' l_k T_k(x'),$$

$$G(x') = \sum_{k=0}^{N_C-1}{}' g_k T_k(x'), \qquad C(x') = \sum_{k=0}^{N_C-1}{}' c_k T_k(x'),$$

$$V(x') = \sum_{k=0}^{\infty}{}' v_k T_k(x') \quad (4a), \qquad I(x') = \sum_{k=0}^{\infty}{}' i_k T_k(x') \quad (4b),$$

$$\frac{dV}{dx'} = \sum_{k=0}^{\infty}{}' v_k^* T_k(x') \quad (5a), \qquad \frac{dI}{dx'} = \sum_{k=0}^{\infty}{}' i_k^* T_k(x') \quad (5b).$$

The prime on the summation symbol means that the first term should be halved before beginning to sum. The expansion coefficients for the voltage (current) derivative v_k^* (i_k^*) are related to the expansion coefficients for the voltage (current) v_k (i_k) by [13]

$$v_k = \frac{1}{2k}\left[v_{k-1}^* - v_{k+1}^*\right] \quad (6a), \qquad i_k = \frac{1}{2k}\left[i_{k-1}^* - i_{k+1}^*\right] \quad (6b)$$

for k=1, 2, ..., ∞. Defining the vectors (of length N_C)

$$\mathbf{v} = \begin{bmatrix}v_1 & v_2 & \cdots & v_{N_C}\end{bmatrix}^T, \qquad \mathbf{v}^* = \begin{bmatrix}v_0^* & v_1^* & \cdots & v_{N_C-1}^*\end{bmatrix}^T,$$

similarly defining $\mathbf{i}$ and $\mathbf{i}^*$, and truncating the expansions in (4) after N_C terms and those in (5) after N_C-1 terms, (6) can be expressed in convenient matrix form:

$$\mathbf{v} = \mathbf{Q}_D\mathbf{v}^* \quad (7a), \qquad \mathbf{i} = \mathbf{Q}_D\mathbf{i}^* \quad (7b)$$

where $\mathbf{Q}_D$ is an N_CXN_C square matrix with the following entries for ith row and jth column

$$\mathbf{Q}_D(i,j) = \begin{cases}\frac{1}{2i} & \text{for } j = i\\ -\frac{1}{2i} & \text{for } j = i+2\\ 0 & \text{otherwise}\end{cases} \quad \text{for i, j = 1, 2, ..., } N_C.$$

Using boundary voltage at $x' = -1$ and boundary current at $x' = +1$, respectively, from (4) and invoking the properties $T_k(+1)=1$ and $T_k(-1) = (-1)^k$ one obtains

$$V(x') = V(-1) + \sum_{k=1}^{N_C} v_k\left[T_k(x') - (-1)^k\right] \tag{8a}$$

$$I(x') = I(+1) + \sum_{n=1}^{N_C} i_k\left[T_k(x') - 1\right]. \tag{8b}$$

Inserting these, the truncated expansions for the derivatives from (5), and the expansions for the line parameters into (2) leads to:

$$\sum_{i=0}^{N_C-1}{}' v_i^* T_i(x') = -\frac{1}{2}\ell * \sum_{i=0}^{N_C-1}{}' \sum_{j=1}^{N_C}(r_i + sl_i)\, i_j\left[\frac{1}{2}T_{i+j}(x') + \frac{1}{2}T_{|i-j|}(x') - T_i(x')\right] - \frac{1}{2}\ell I(+1)\sum_{i=0}^{N_C-1}{}'(r_i + sl_i)T_i(x') \quad \text{and} \tag{9a}$$

$$\sum_{i=0}^{N_C-1}{}' i_i^* T_i(x') = -\frac{1}{2}\ell \sum_{i=0}^{N_C-1}{}' \sum_{j=1}^{N_C}(g_i + sc_i)\, v_j\left[\frac{1}{2}T_{i+j}(x') + \frac{1}{2}T_{|i-j|}(x') - (-1)^j T_i(x')\right] - \frac{1}{2}\ell V(-1)\sum_{i=0}^{N_C-1}{}'(g_i + sc_i)T_i(x'), \tag{9b}$$

where use has been made of the triple-recursion formula [14]

$T_i(x')T_j(x') = \frac{1}{2}\left[T_{i+j}(x') + T_{|i-j|}(x')\right]$. Taking the Chebyshev inner product $\langle \cdot\,, T_k(x')\rangle$ for k=0,1,..., N_C on both sides of (14) and noting that [14]

$$\left\langle T_m(x'),\, T_n(x')\right\rangle = \begin{cases} 0 & m \neq n \\ \pi & m = n = 0 \\ \pi/2 & m = n > 0 \end{cases}$$

one obtains $2N_C$ linear algebraic equations in matrix form:

$$\mathbf{v}^* = (\mathbf{X}_R + s\mathbf{X}_L)\mathbf{i} - (\mathbf{E}_R + s\mathbf{E}_L)I(+1) \tag{10a}$$

$$\mathbf{i}^* = (\mathbf{X}_G + s\mathbf{X}_C)\mathbf{v} - (\mathbf{E}_G + s\mathbf{E}_C)V(-1), \tag{10b}$$

where $\mathbf{X}_R(i,j) = \frac{1}{2}\ell\left[\pi_{i-1} - \frac{1}{2}\left(\pi_{i+j-1} + \pi_{|i-j-1|}\right)\right]$,

$\mathbf{X}_C(i,j) = \frac{1}{2}\ell\left[(-1)^j\alpha_{i-1} - \frac{1}{2}\left(\alpha_{i+j-1} + \alpha_{|i-j-1|}\right)\right]$

for i, j = 1, 2, ..., N_C, $\mathbf{X}_L$ is defined similar to $\mathbf{X}_R$, $\mathbf{X}_G$ is defined similar to $\mathbf{X}_C$,

$$\mathbf{E}_R = \frac{1}{2}\ell\left[\pi_0 \quad \pi_1 \quad \pi_2 \quad \cdots \quad \pi_{N_C-1}\right]^T$$

and $\mathbf{E}_L$, $\mathbf{E}_G$, $\mathbf{E}_C$ are similarly defined.

Equations (10a) and (10b) can be expressed in compact form:

$$\begin{bmatrix}\mathbf{v}^* \\ \mathbf{i}^*\end{bmatrix} = \left(\mathbf{X}_{RG} + s\mathbf{X}_{LC}\right)\begin{bmatrix}\mathbf{v} \\ \mathbf{i}\end{bmatrix} - \left(\mathbf{E}_{RG} + s\mathbf{E}_{LC}\right)\begin{bmatrix}V(-1) \\ I(+1)\end{bmatrix} \tag{11}$$

where $\mathbf{X}_{RG} = \begin{bmatrix}\mathbf{0} & \mathbf{X}_R \\ \mathbf{X}_G & \mathbf{0}\end{bmatrix}$; $\mathbf{X}_{LC} = \begin{bmatrix}\mathbf{0} & \mathbf{X}_L \\ \mathbf{X}_C & \mathbf{0}\end{bmatrix}$;

$\mathbf{E}_{RG} = \begin{bmatrix}\mathbf{0} & \mathbf{E}_R \\ \mathbf{E}_G & \mathbf{0}\end{bmatrix}$; $\mathbf{E}_{LC} = \begin{bmatrix}\mathbf{0} & \mathbf{E}_L \\ \mathbf{E}_C & \mathbf{0}\end{bmatrix}$.

Equations (7) and (11) can be readily solved to obtain the expansion coefficients for the line voltage and current:

$$\begin{bmatrix}\mathbf{v} \\ \mathbf{i}\end{bmatrix} = \left\{s\mathbf{X}_{LC} - (\mathbf{Q} - \mathbf{X}_{RG})\right\}^{-1}\left(\mathbf{E}_{RG} + s\mathbf{E}_{LC}\right)\begin{bmatrix}V(-1) \\ I(+1)\end{bmatrix}, \tag{12}$$

where $\mathbf{Q} = \begin{bmatrix}\mathbf{Q}_D^{-1} & \mathbf{0} \\ \mathbf{0} & \mathbf{Q}_D^{-1}\end{bmatrix}$.

Using boundary values V(+1) and I(-1) from (8) and noting that $T_k(+1)=1$ and $T_k(-1) = (-1)^k$ one obtains

$$\begin{bmatrix}V(+1) \\ I(-1)\end{bmatrix} = \begin{bmatrix}V(-1) \\ I(+1)\end{bmatrix} + \mathbf{F}\begin{bmatrix}\mathbf{v} \\ \mathbf{i}\end{bmatrix}, \tag{13}$$

where $\mathbf{F} = \begin{bmatrix}\mathbf{P} & \mathbf{0} \\ \mathbf{0} & -\mathbf{P}\end{bmatrix}$ and P is a row-vector of length N_C:

$$\mathbf{P} = \begin{bmatrix}2 & 0 & 2 & \cdots & 1-(-1)^{N_C}\end{bmatrix}.$$

Substituting (12) into (13) finally yields

$$\begin{bmatrix}V(+1) \\ I(-1)\end{bmatrix} = \mathbf{H}(s)\begin{bmatrix}V(-1) \\ I(+1)\end{bmatrix} \text{ with} \tag{14}$$

$$\mathbf{H}(s) = \mathbf{U}_2 + \mathbf{F}\left\{s\mathbf{X}_{LC} - (\mathbf{Q} - \mathbf{X}_{RG})\right\}^{-1}\left(\mathbf{E}_{RG} + s\mathbf{E}_{LC}\right),$$

where $\mathbf{U}_2$ is a unit matrix of order 2. Straightforward manipulations yields

$$\mathbf{H}(s) = \mathbf{D} + \mathbf{C}(s\mathbf{U}_{2N_C} - \mathbf{A})^{-1}\mathbf{B}, \tag{15}$$

where $\mathbf{A} = (\mathbf{Q} - \mathbf{X}_{RG})\mathbf{X}_{LC}^{-1}$, $\mathbf{B} = \mathbf{E}_{RG} + \mathbf{A}\mathbf{E}_{LC}$

$\mathbf{C} = \mathbf{F}\mathbf{X}_{LC}^{-1}$, and $\mathbf{D} = \mathbf{U}_2 + \mathbf{F}\mathbf{X}_{LC}^{-1}\mathbf{E}_{LC}$.

Here, use has been made of the identity:

$$s(s\mathbf{U}_{2N_C} - \mathbf{A})^{-1} = \mathbf{U}_{2N_C} + \mathbf{A}(s\mathbf{U}_{2N_C} - \mathbf{A})^{-1}$$

$$= \mathbf{U}_{2N_C} + (s\mathbf{U}_{2N_C} - \mathbf{A})^{-1}\mathbf{A}$$

One can immediately notice the similarity between (15) and the transfer-function matrix of a linear time-invariant system described in the classical state-variable form, with $\mathbf{A}$ being the state-transition matrix. $\mathbf{D}$ represents the direct transmission term and is the high-frequency limiting value of the h-parameter matrix since the remaining term of $\mathbf{H}(s)$ is a strictly proper rational function which tends to zero as $s \to \infty$.

2.2. Hybrid parameters of a multiconductor transmission line

The h-parameter matrix of a multiconductor line can be computed in a manner analogous to the one for a single-conductor line. In this case, however, the following column vectors of length $N*N_C$ will replace the corresponding quantities for the single-conductor case:

$$\mathbf{v} = \begin{bmatrix}\mathbf{v}_1 \\ \mathbf{v}_2 \\ \vdots \\ \mathbf{v}_N\end{bmatrix}; \quad \mathbf{i} = \begin{bmatrix}\mathbf{i}_1 \\ \mathbf{i}_2 \\ \vdots \\ \mathbf{i}_N\end{bmatrix}; \quad \mathbf{v}^* = \begin{bmatrix}\mathbf{v}_1^* \\ \mathbf{v}_2^* \\ \vdots \\ \mathbf{v}_N^*\end{bmatrix}; \quad \mathbf{i}^* = \begin{bmatrix}\mathbf{i}_1^* \\ \mathbf{i}_2^* \\ \vdots \\ \mathbf{i}_N^*\end{bmatrix}$$

The nth entries of $\mathbf{v}$ ($\mathbf{i}$) and $\mathbf{v}^*$ ($\mathbf{i}^*$), respectively, contains the expansion coefficients of the voltage (current) on the nth conductor $V_n(x')$ ($I_n(x')$), and its derivative:

$$\mathbf{v}_n = \begin{bmatrix}v_{n,1} & v_{n,2} & \cdots & v_{n,N_C}\end{bmatrix}^T;$$

$$\mathbf{v}_n^* = \begin{bmatrix}v_{n,0}^* & v_{n,1}^* & \cdots & v_{n,N_C-1}^*\end{bmatrix}^T$$

$$\mathbf{i}_n = \begin{bmatrix}i_{n,1} & i_{n,2} & \cdots & i_{n,N_C}\end{bmatrix}^T;$$

$$\mathbf{i}_n^* = \begin{bmatrix}i_{n,0}^* & i_{n,1}^* & \cdots & i_{n,N_C-1}^*\end{bmatrix}^T.$$

Following the same procedure as in the case of a single conductor results in an expression in the state-space form which is identical to the expression (22). The derivation will not be presented here due to space limitation. It is to be noted, however, that the dimensions of $\mathbf{A}$, $\mathbf{B}$, $\mathbf{C}$, and $\mathbf{D}$ are, respectively, $2N*N_C$X$2N*N_C$, $2N*2N_C$X$2N$, $2N$X$2N*N_C$, $2N$X$2N$.

III. TIME-DOMAIN MACROMODEL

The time-domain description of the transmission line, corresponding to the frequency-domain relation (3), may be expressed by the convolution integral:

$$\begin{bmatrix}\mathbf{v}(+1,\,t) \\ \mathbf{i}(-1,\,t)\end{bmatrix} = \mathbf{h}(t) * \begin{bmatrix}\mathbf{v}(-1,\,t) \\ \mathbf{i}(+1,\,t)\end{bmatrix} = \int_0^t \mathbf{h}(t-\tau)\begin{bmatrix}\mathbf{v}(-1,\,\tau) \\ \mathbf{i}(+1,\,\tau)\end{bmatrix} d\tau, \tag{16}$$

where $\mathbf{h}(t)$ (the impulse-response matrix) is the time-domain inverse of $\mathbf{H}(s)$. To facilitate efficient recursive evaluation of convolution, $(s\mathbf{U}_{2N_C} - \hat{\mathbf{A}})^{-1}$ in (15) is expressed as [15]

$$(s\mathbf{U}_{2N_C} - \hat{\mathbf{A}})^{-1} = \sum_{k=1}^{2N_C} \frac{1}{s-\lambda_k}\mathbf{q}_k\mathbf{p}_k, \qquad (17)$$

where q_k and P_k are, respectively, right and left eigenvectors of $\hat{\mathbf{A}}$ associated with the eigenvalue λ_k. It is to be noted that q_k is a column vector and P_k is a row vector of length $2N_C$, and

$$\begin{bmatrix} \mathbf{p}_1 \\ \mathbf{p}_2 \\ \vdots \\ \mathbf{p}_{2N_C} \end{bmatrix} = \begin{bmatrix} \mathbf{q}_1 & \mathbf{q}_2 & \cdots & \mathbf{q}_{2N_C} \end{bmatrix}^{-1}.$$

Substituting (17) into (15) leads to the rational function expansion of $\mathbf{H}(s)$ in partial fraction form:

$$\mathbf{H}(s) = \hat{\mathbf{D}} + \sum_{k=1}^{2N_C} \frac{1}{s-\lambda_k}\mathbf{k}_k, \qquad (18)$$

where $\mathbf{k}_k = \hat{\mathbf{C}}\mathbf{q}_k\mathbf{p}_k\hat{\mathbf{B}}$ is the kth residue matrix corresponding to the pole λ_k. An important feature of the rational function expansion (18) is that all the entries of $\mathbf{H}(s)$ have the same set of poles. This common denominator property, which is a natural outcome of the formulation, simplifies the transient simulation routine and greatly reduces the computational effort. The impulse response matrix is readily obtained as

$$\mathbf{h}(t) = \hat{\mathbf{D}}\delta(t) + \sum_{k=1}^{2N_C} \exp(\lambda_k t)\mathbf{k}_k. \qquad (19)$$

In a transient simulation scheme, it is convenient to assume the port voltage and current waveforms as linear functions of time between successive time steps. The convolution integration from time point t to $t+\Delta t$ of the piecewise-linear port variables with the impulse response function (19) may then be carried out analytically yielding the recursive formulation:

$$\begin{bmatrix} v(+1,\, t+\Delta t) \\ i(-1,\, t+\Delta t) \end{bmatrix} = h\begin{bmatrix} v(-1,\, t+\Delta t) \\ i(+1,\, t+\Delta t) \end{bmatrix} + \sum_{k=1}^{2N_C} c_k(t+\Delta t) \qquad (20)$$

where $$\mathbf{h} = \hat{\mathbf{D}} + \sum_{k=1}^{2N_C} \beta_k\mathbf{k}_k, \qquad (21)$$

$$\mathbf{c}_k(t+\Delta t) = \exp(\lambda_k\Delta t)\mathbf{f}_k(t) + \alpha_k\mathbf{k}_k\begin{bmatrix} \mathbf{v}(-1,\, t) \\ \mathbf{i}(+1,\, t) \end{bmatrix},$$

and $$\mathbf{f}_k(t+\Delta t) = \mathbf{c}_k(t+\Delta t) + \beta_k\mathbf{k}_k\begin{bmatrix} \mathbf{v}(-1,\, t+\Delta t) \\ \mathbf{i}(+1,\, t+\Delta t) \end{bmatrix}$$

with $$\alpha_k = \frac{1}{\lambda_k}\left[\frac{\exp(\lambda_k\Delta t)-1}{\lambda_k\Delta t} - 1\right] \text{ and}$$

$$\beta_k = \frac{1}{\lambda_k}\left[\exp(\lambda_k\Delta t) + \frac{1-\exp(\lambda_k\Delta t)}{\lambda_k\Delta t}\right].$$

Recursive convolution is effected by updating the vectors $\mathbf{f}_k$'s at each time point by using the port voltages and currents obtained from the solution of the combined linear and nonlinear circuit. Equation (20) is amenable to the development of Thevenin and Norton type time-varying circuit model representation of the transmission line. In an MNA formulation for the network equations, (20) needs to be manipulated before being assimilated into the global MNA matrix. These manipulations permit one to express the MNA stamp for the transmission line as

$$\begin{bmatrix} i(-1,\, t+\Delta t) \\ i(+1,\, t+\Delta t) \end{bmatrix} = y\begin{bmatrix} v(-1,\, t+\Delta t) \\ v(+1,\, t+\Delta t) \end{bmatrix} + \sum_{k=1}^{2N_C} i_{ok}(t+\Delta t) \qquad (22)$$

where $$\mathbf{i}_{ok}(t+\Delta t) = \exp(\lambda_k\Delta t)\mathbf{f}_{ok}(t) + \alpha_k\mathbf{T}\mathbf{k}_k\begin{bmatrix} \mathbf{v}(-1,\, t) \\ \mathbf{i}(+1,\, t) \end{bmatrix},$$

$$\mathbf{f}_{ok}(t+\Delta t) = \mathbf{i}_{ok}(t+\Delta t) + \beta_k\mathbf{T}\mathbf{k}_k\begin{bmatrix} \mathbf{v}(-1,\, t+\Delta t) \\ \mathbf{i}(+1,\, t+\Delta t) \end{bmatrix},$$

$$\mathbf{y} = \begin{bmatrix} \mathbf{h}_{21} - \mathbf{h}_{22}\mathbf{h}_{12}^{-1}\mathbf{h}_{11} & \mathbf{h}_{22}\mathbf{h}_{12}^{-1} \\ -\mathbf{h}_{12}^{-1}\mathbf{h}_{11} & \mathbf{h}_{12}^{-1} \end{bmatrix}, \quad \mathbf{T} = \begin{bmatrix} -\mathbf{h}_{22}\mathbf{h}_{12}^{-1} & \mathbf{U}_N \\ -\mathbf{h}_{12}^{-1} & \mathbf{0} \end{bmatrix}.$$

Here, $\mathbf{h}_{ij}$ (i, j = 1 or 2) are NXN submatrices of the 2NX2N matrix $\mathbf{h}$ defined in (21). The circuit models, based on (21), have been implemented in a prototype transient analyzer for interconnect networks (TRAIN). The trapezoidal algorithm of numerical integration is used to derive time-varying Norton equivalents for the reactive elements. These linear one-port models consist of constant resistances and time-varying voltage or current sources computed and updated at each time point. An iteration scheme based on Newton-Raphson algorithm is used to linearize nonlinear elements. The transient simulation proceeds in a time marching fashion. At each time step t, a linear system of equations is solved iteratively and the solution is then used to update the time-varying current sources so that the transient analysis can be carried out at time step $t+\Delta t$.

IV. EXAMPLES AND NUMERICAL CONSIDERATIONS

To illustrate the accuracy, efficiency and versatility of the proposed method, results for representative circuits are presented and compared, where possible, with the results given by the simulator SPICE3E. All CPU times are for an IBM RS6000/530 machine.

The first example involves a single-conductor parabolic RLC line with $R(x)=Ro(1+ax)^2$, $L(x)=Lo(1+ax)^2$ and $C(x)=Co(1+ax)^2$, where $Ro=3\Omega/cm$, $Lo=2.5nH/cm$ and $Co=1pF/cm$. The line has a length of 10 cm and a tapering factor $1+a\ell=\sqrt{2}$. It is driven by a CMOS inverter ($\beta n=7.5X10^{-3}$, $\beta p=7.5X10^{-3}$ and $Vtn=|Vtp|=1V$) and is terminated in a 0.5 pF capacitor. The nonuniform transmission line was modeled in SPICE3E by a cascaded network of 10 uniform RLC lines. The output voltage responses due to a trapezoidal input waveform of 5 ns pulse width and 0.2 ns rise/fall time are compared in Fig. 1. The agreement between the two results is excellent. The number of terms (N_C) in Chebyshev series used in TRAIN was 15 and the step size was $\Delta t = 25$ ps. The CPU time for TRAIN simulation was 0.8 s and that for SPICE3E simulation (REL=1) was 66 s.

Fig. 2 shows the TRAIN output waveforms for the parabolic line computed using different order of approximations N_C=7, 10 and 15. The step size Δt =25 ps for the three simulations. The

three waveforms are almost identical except in the vicinities of the fast-varying portions where the waveform is characterized by oscillations when N_C is small. In general, increasing the order of approximation has two effects: the low-frequency poles are computed more accurately and additional high-frequency poles are generated that enhances the high-frequency details of the estimated waveforms. A value of N_C greater than 15 will hardly be necessary for the present-day speed requirements in digital circuits. The proper choice of the approximation order will be dictated by the application, the time step used in transient simulation, and the expected nature, such as presence or absence of sharp edges, of the waveforms.

The next example is intended to demonstrate the generality of the proposed method. A tri-conductor nonuniform coupled lossy line was simulated by TRAIN. The geometry and the terminations of the microstrip structure is shown in Fig. 3. **L** and **C** matrices, as a function of distance, were computed using the software tool CAP2D [16]. The spatial dependence of **R** matrix was taken into account by considering the resistance to vary inversely with the conductor width. Least-square polynomial for each entry of the parameter matrices was computed and the Chebyshev expansion was then evaluated analytically from this fitted polynomial. For a kth order interpolating polynomial, the Chebyshev expansion does not involve terms of order (k+1) or higher. This two-step approach of determining the Chebyshev coefficients gives better accuracy than the direct integration approach or the FFT technique. The source signals on the active-line is a pulse with 4.0 ns pulse-width and 0.1 ns rise/fall time. A pair of crosstalk waveforms on the nearby quite-lines are shown in Fig. 4.

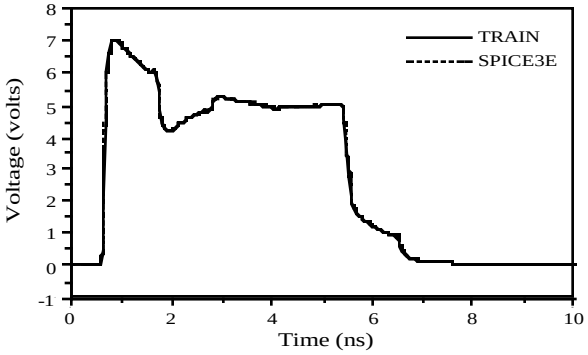

Fig. 1. Output voltage waveform of a parabolic line.

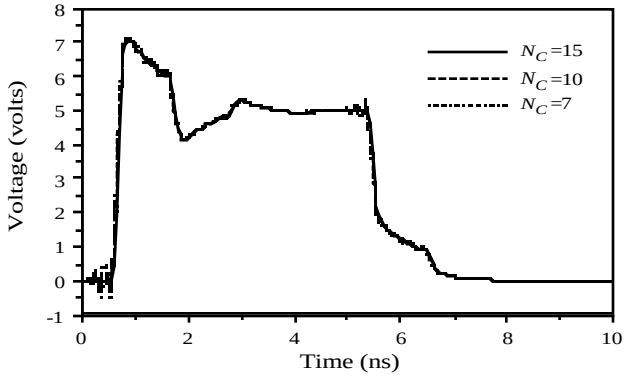

Fig. 2. Output Voltage waveforms of the parabolic line for different values of N_C.

A time step of 25 ps and N_C=15 were used. The total simulation time was 2.8 s. The time required to create the macromodel was 1.2 s.

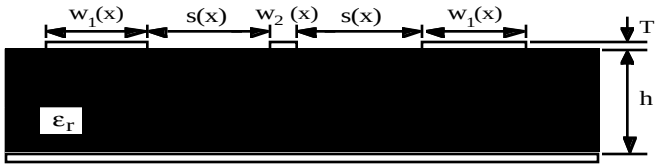

T=1μm, σ =3.5x10-7/Ω-m, h=0.635 mm and ε_r=10

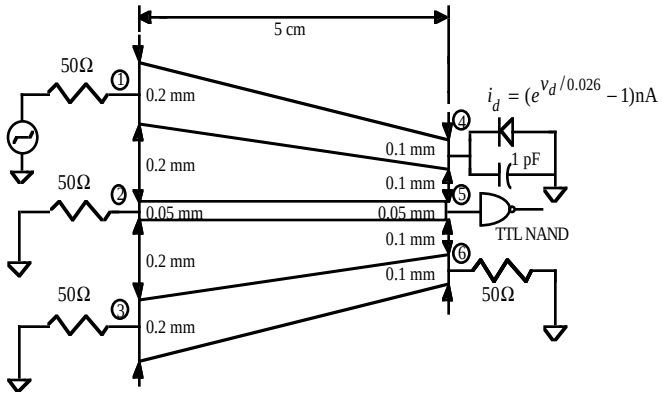

(a)

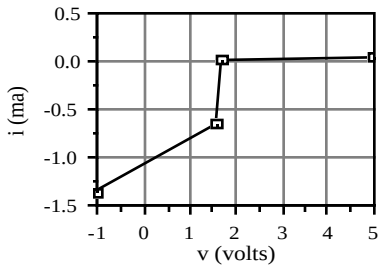

(b)

Fig. 3. (a) Geometry and terminations of a nonuniform microstrip configuration. (b) I-V characteristics of the TTL NAND gate used as an inverter.

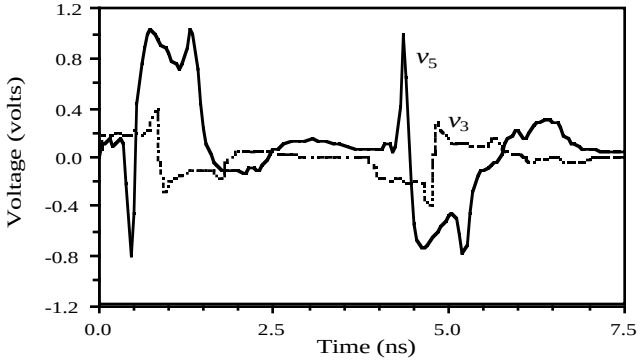

Fig. 4. Crosstalk for the network in Fig. 3.

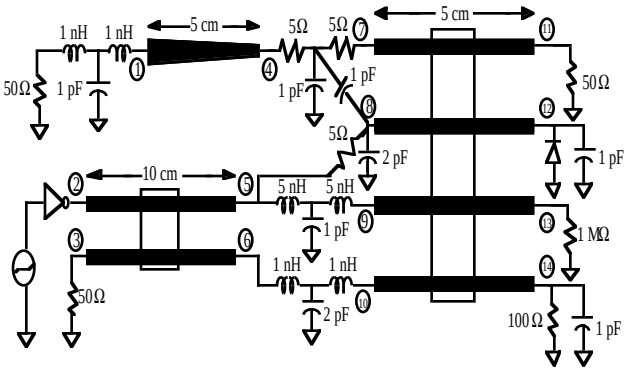

Fig. 5. A circuit containing coupled uniform and uncoupled nonuniform line.

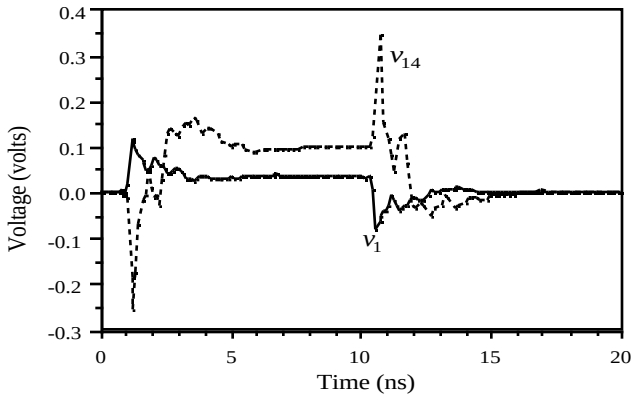

Fig. 6. Voltage signals at nodes 1 and 14 of the circuit in Fig. 5.

In the final example, TRAIN was used to simulate the circuit shown in Fig. 5. It contains two systems of coupled uniform RLCG lines and a single nonuniform RLCG line. The per-unit-length parameters for the uniform lines were taken from [7]. The nonuniform line, on a 10 μm thick SiO_2 substrate, has a conductor thickness of 2 μm and a width that varies linearly from 33 μm to 11 μm. The per-unit-length conductance for the nonuniform line is assumed constant at G=0.1 S/m. The CMOS inverter is excited by a pulse with a 10 ns width and 0.5 ns rise/fall time. The voltage waveforms at two nodes of the circuit, computed by TRAIN using a 50 ps time step, are shown in Fig. 6. The computation of the macromodels with N_C=10 required 1.7 CPU s and the transient analysis of the circuit consumed an additional 4.2 CPU s.

V. CONCLUSIONS

A time-domain macromodel based on the h-parameter description of a general interconnect structure has been derived. The derivation is based on the spectral method solution of the telegrapher equations and a recursive convolution algorithm. The macromodel can be directly stenciled into the MNA matrix of the overall circuit. Simulation results on uniform and nonuniform structures terminated in linear and nonlinear elements have been presented to demonstrate the accuracy, efficiency and generality of the derived macromodel. These and other experimental results suggest that the model is unconditionally stable. A rigorous treatment of the stability issue showing that all eigenvalues of the matrix $\mathbf{A}'$ are negative is of interest. Future research will also include the extension of the approach to transmission lines with frequency-dependent parameters.

REFERENCES

[1] A. R. Djordjevic, T. K. Sarkar, and R. F. Harrington, "Analysis of lossy transmission lines with arbitrary nonlinear terminal networks," *IEEE Trans. Microwave Theory Tech.*, vol. 34, pp. 660-665, June 1986.

[2] J. E. Schutt-Aine and R. Mittra, "Nonlinear transient analysis of coupled transmission lines," *IEEE Trans. Circuits Syst.*, vol. 36, pp. 959-967, July 1989.

[3] J. R. Griffith and M. S. Nakhla, "Time-domain analysis of lossy coupled transmission lines,"*IEEE Trans. Microwave Theory Tech.*, vol. 38, pp.1480-1487, Oct. 1990.

[4] D. Winklestein, M. B. Steer, and R. Pomerleau, "Simulation of arbitrary transmission line network with nonlinear terminations," *IEEE Trans. Circuits Syst.*, vol. 38, pp. 418-412, April 1991.

[5] J. S. Roychowdhury and D. O. Pederson, "Efficient transient simulation of lossy interconnect," in *Proc. 28th Design Automation Conf.*, pp. 740-745, June 1991.

[6] A. Semlyen and A. Dabuleanu, "Fast and accurate switching transient calculation on transmission lines with ground return using recursive convolution," *IEEE Trans. Power App. Syst.*, vol. 94. pp. 561-571, 1975.

[7] T. K. Tang and M. S. Nakhla, "Analysis of high-speed VLSI interconnects using the Asymptotic Waveform Evaluation technique," *IEEE Trans. Computer-Aided Design*, vol. 11, pp. 341-352, March 1992.

[8] J. E. Bracken, V. Raghavan, and R. A. Rohrer, "Interconnect simulation with Asymptotic Waveform Evaluation," *IEEE Trans. Circuits and Syst.*, vol. 39, pp. 869-878, Nov. 1992.

[9] S. Lin and E. Kuh, "Transient simulation of lossy interconnects based on the recursive convolution formulation," *IEEE Trans. Circuits and Syst.*, vol. 39, pp. 879-892, Nov. 1992.

[10] R. Griffith, E. Chiprout, and M. S. Nakhla, "A CAD framework for simulation and optimization of high-speed VLSI interconnections," *IEEE Trans. Circuits and Syst.*, vol. 39, pp. 893-906, Nov. 1992.

[11] E. Chiprout and M. S. Nakhla, "Transient waveform estimation of high-speed MCM networks using complex frequency hopping," in *Proc. Multi-Chip Module Conf.*, March 1993.

[12] F. Y. Chang, "Transient simulation of nonuniform coupled lossy transmission lines characterized with frequency-dependent parameters, Part II: discrete-time analysis," *IEEE Trans. Circuits and Syst.*, vol. 39, pp. 907-927, Nov. 1992.

[13] O. A. Palusinski and A. Lee, "Analysis of transients in nonuniform and uniform multiconductor transmission lines," *IEEE Trans. Microwave Theory Tech.*, vol. 37, pp. 127-138, Jan. 1989.

[14] K. E. Atkinson, *An Introduction to Numerical Analysis*, 2nd ed. New York: John Wiley & Sons, 1989, ch. 4.

[15] C. T. Chen, *Linear System Theory and Design*. Holt, Rineheart and Winston, Inc., 1984, ch. 2.

[16] C. P. Yuan, *Modeling and extraction of interconnect parameters in very-large-scale integrated circuits*, Ph. D. dissertation, Univ. of Illinois at Urbana-Champaign, August 1983.